

1 **Description and Validation of the Colorectal Cancer and Adenoma Incidence &**  
2 **Mortality (CRC-AIM) Microsimulation Model**

3

4 **Running Title:** CRC-AIM: CRC and Adenoma Microsimulation Model

5

6 Andrew Piscitello, MAT<sup>1\*</sup> ([ajpiscitello@gmail.com](mailto:ajpiscitello@gmail.com)), Leila Saoud, MS<sup>2</sup>

7 ([Isaoud@exactsciences.com](mailto:Isaoud@exactsciences.com)), Michael Matney, MS<sup>2</sup> ([mmatney@exactsciences.com](mailto:mmatney@exactsciences.com)),

8 Bijan J Borah, PhD<sup>3</sup> ([Borah.bijan@mayo.edu](mailto:Borah.bijan@mayo.edu)), A Mark Fendrick, MD<sup>4</sup>

9 ([amfen@umich.edu](mailto:amfen@umich.edu)), Kristen Hassmiller Lich, PhD, MHSA<sup>5</sup> ([klich@unc.edu](mailto:klich@unc.edu)), Harald

10 Rinde, MD, MBA<sup>6</sup> ([harald@rinde.com](mailto:harald@rinde.com)), Paul J Limburg, MD<sup>7</sup> ([Limburg.paul@mayo.edu](mailto:Limburg.paul@mayo.edu))

11

12 1. EmpiriQA LLC, 1580 Roanoke Court, Long Grove, IL 60047

13 2. Exact Sciences Corporation, 441 Charmany Drive, Madison, WI 53719

14 3. Division of Health Care Policy & Research, Mayo Clinic, 200 First St. SW,  
15 Rochester, MN 55905

16 4. Division of General Internal Medicine, Department of Internal Medicine, University of  
17 Michigan, 2800 Plymouth Rd, Bldg 16, Floor 4, 016-400S-25, Ann Arbor, MI 48109

18 5. Department of Health Policy & Management, University of North Carolina at Chapel  
19 Hill, 1105E McGavran-Greenberg Hall, CB #7411, Chapel Hill, NC 27599

20 6. BioBridge Strategies, 12 Bd Princesse Charlotte, 98000 Monaco

21 7. Division of Gastroenterology and Hepatology, Mayo Clinic, 200 First St. SW,  
22 Rochester, MN 55905

23

24 \*Corresponding author

25

26 **Word Count:** 6409

27 **Abstract**

28 *Background:* Microsimulation models of colorectal cancer (CRC) have helped  
29 inform national screening guidelines and health policy decision-making. However,  
30 detailed descriptions of particular underlying assumptions are not published, limiting  
31 access to robust platforms for exploratory analyses. We describe the development and  
32 validation of the Colorectal Cancer and Adenoma Incidence and Mortality (CRC-AIM)  
33 microsimulation model, a robust model built to facilitate collaborative simulation studies  
34 on disease progression and early detection through screening interventions.

35 *Design:* We used the Cancer Intervention and Surveillance Modeling Network  
36 (CISNET) CRC models, specifically CRC-SPIN, as a foundation for CRC-AIM's  
37 formulas and parameters. In addition, we developed novel submodels and recalibrated  
38 various parameters to address gaps and discrepancies in publicly available information.  
39 Along with evaluating the natural history and screening detection outcomes from CRC-  
40 AIM, we determined the impact of using different life tables (cohort versus period) on  
41 natural history outcomes.

42 *Results:* CRC-AIM demonstrated substantial cross-model validity when  
43 comparing multiple natural history and screening outputs and probability curves to those  
44 from CISNET models, particularly CRC-SPIN. Additionally, using period life tables,  
45 CRC-AIM's cumulative probability of developing CRC from ages 40 to 100 (7.1%) lies  
46 within the range of the CISNET models (6.7% to 7.2%). Using cohort tables, that  
47 probability increases to 8.0%. One notable difference is that, regardless of life table  
48 used, the cumulative probability of dying from CRC (3.2% for period; 3.8% for cohort) is  
49 slightly higher in CRC-AIM than the CISNET models (2.7% to 2.8%), due to CRC-AIM's

50 different methodology for determining survival. Additionally, there is substantial overlap  
51 (e.g. 94-95% overall agreement for strategies on and off the efficient frontier for stool-  
52 based strategies) across multiple screening overlay outputs between CRC-AIM and the  
53 CISNET models, especially CRC-SPIN.

54 *Conclusions:* We developed and validated a robust CRC microsimulation model,  
55 CRC-AIM, and demonstrate the influence of life table choice on downstream outputs.  
56 We further describe CRC-AIM's parameters and include complete component tables to  
57 enhance transparency and encourage collaboration.

## 58 **Introduction**

59           The U.S. Preventive Services Task Force (USPSTF), an independent panel of  
60 national experts in disease prevention and evidence-based medicine, supplement  
61 empirical data with microsimulation models to inform national preventive and screening  
62 guidelines. For colorectal cancer (CRC), the USPSTF relies on information such as  
63 model outputs from the Cancer Intervention and Surveillance Modeling Network  
64 (CISNET) Colorectal Working Group (CWG). The CWG comprises a coordinating center  
65 and three independent modeling groups: (1) the Colorectal Cancer Simulated  
66 Population model for Incidence and Natural history (CRC-SPIN) from the RAND  
67 Corporation; (2) the Simulation Model of Colorectal Cancer (SimCRC) from the  
68 University of Minnesota; and (3) Microsimulation Screening Analysis (MISCAN) from  
69 Memorial Sloan Kettering and Erasmus University, Rotterdam.<sup>1,2</sup>

70           These highly sophisticated microsimulation models are powerful tools to simulate  
71 the complicated natural history of CRC and precursor lesions in individual patients and  
72 identify effective screening interventions for the early detection of CRC.<sup>3-5</sup> Over time, the  
73 model components have evolved and been recalibrated and reparametrized with the  
74 emergence of new clinical data (eg, CRC-SPIN v2.x<sup>6</sup>). Although CISNET has  
75 documented many changes to the models throughout the years, due to their complexity,  
76 it can be difficult to fully determine the downstream effects of recalibration based only  
77 on publicly accessible information.<sup>5</sup>

78           To provide additional transparency and generate an alternative platform for  
79 collaborative modeling analyses, we created a robust microsimulation model—the  
80 Colorectal Cancer and Adenoma Incidence & Mortality (CRC-AIM) microsimulation

81 model—based on previously reported parameters from CRC-SPIN.<sup>7</sup> We selected CRC-  
82 SPIN as a foundational natural history model because of its comparatively high degree  
83 of parsimony, documentation and transparency. Nevertheless, complete details of  
84 various components of CRC-SPIN, such as the submodel to determine CRC stage  
85 based on size, could not be found in the published literature. This required us to make  
86 informed assumptions and create additional submodels to produce a functioning  
87 microsimulation model. (See **Supplementary Material** for a detailed description of the  
88 differences between CRC-AIM and CRC-SPIN.)

89 In this publication, we describe the methods used to develop CRC-AIM and  
90 demonstrate its robustness by thoroughly comparing its outputs to the published natural  
91 history and screening outputs of the three CISNET CWG models (CRC-SPIN, SimCRC,  
92 and MISCAN). Furthermore, we examine the consequence of selecting different life  
93 tables on natural history outputs. The CISNET models use period life tables, which may  
94 underestimate survival because they only describe mortality conditions at a particular  
95 time.<sup>1,8</sup> We explore the consequences of cohort life tables, which build in differential risk  
96 across generations by assuming improved mortality rates over time.<sup>8,9</sup> The CRC-AIM  
97 microsimulation model can help inform and address long-standing clinical questions,  
98 such as exploring alternate surveillance scenarios and varied colonoscopy performance  
99 data.

100 Ultimately, CRC-AIM not only demonstrates the approach by which existing CRC  
101 models can be reproduced from publicly available information, but also provides a ready  
102 opportunity for interested researchers to leverage the model for future collaborative  
103 projects or further adaptation and testing. To promote transparency and credibility of

104 this new model, we have made available CRC-AIM's formulas and parameters on a  
105 public repository (<https://github.com/CRCAIM/CRC-AIM-Public>).

106

## 107 **Methods**

### 108 Natural History

109 Natural history modeling for colorectal cancer (CRC) describes the adenoma-  
110 carcinoma sequence in the absence of screening for a large population of individuals  
111 (**Figure 1**). During one's lifetime, an individual may generate one or more adenomas.  
112 These adenomas independently grow at different rates and may transition into  
113 preclinical CRC. The time between adenoma initiation and its transition to preclinical  
114 cancer is defined as the *adenoma dwell time*, which is different for each adenoma. In  
115 the absence of screening, the time required for a preclinical cancer to become clinically  
116 detected, meaning the appearance of disease signs and symptoms, is defined as the  
117 *sojourn time* (ST) of the cancer. Each preclinical cancer generated in CRC-AIM is  
118 assigned an ST. Upon completion of the ST, the CRC becomes clinically detected and a  
119 CRC survival methodology is used to determine the age of cancer cause-specific  
120 mortality. If multiple preclinical CRCs exist within an individual, the first cancer to  
121 become clinically detected determines survival.<sup>6,10</sup> The cause of death is considered to  
122 be cancer-cause-specific or other-cause-specific, depending on which occurred first in  
123 the simulation.

124 The model simulates all events until an individual reaches their other-cause  
125 mortality date. This approach is analogous to the "parallel universe" model described in  
126 CRC-SPIN.<sup>6,10</sup>

127 See **Supplemental Material** for detailed descriptions of formulas and  
128 assumptions related to CRC-AIM's natural history.

129 *Simulating all-cause mortality*

130 To simulate death from other causes, the CISNET models use period life tables,  
131 which use mortality rates from a particular period in time to represent mortality rates  
132 throughout an individual's lifetime. CRC-AIM, however, uses cohort (generation) life  
133 tables, which determine annual survival from past mortality rates and/or from projected  
134 mortality rates. The cohort life tables provide decennial survival information for cohorts  
135 born between 1900 and 2010 and project mortality for decennial years 2010 through  
136 2100. We interpolate across birth cohort decade to obtain survival estimates for a  
137 specific cohort year and interpolate within a year-of-death interval for specific age at  
138 death. The model uses a birth-year-specific sex ratio based on data from the U.S.  
139 Census Bureau.<sup>11</sup>

140 *Adenoma generation and location*

141 CRC-AIM uses the non-homogenous Poisson process from CRC-SPIN v1.0,  
142 specifically the instantaneous risk function, to generate adenomas in an individual.<sup>10</sup>  
143 Adenoma risk is based on an individual's per-person (inherent) risk, sex, and age. This  
144 process assumes no risk of generating adenomas prior to age 20, after which risk  
145 generally increases with age. Nonadenomatous polyps are not explicitly modeled  
146 because they are not considered to progress to CRC.<sup>12</sup> Adenomas are localized either  
147 to the colon (91% total: 8% cecum, 23% ascending, 24% transverse, 12% descending,  
148 24% sigmoid) or the rectum (9% total), similar to CRC-SPIN v1.0.<sup>10</sup> Location (colon  
149 versus rectum) is used for other natural history components of the model.



150 *Adenoma growth*

151 CRC-AIM uses the adenoma growth function from CRC-SPIN v1.0 to describe  
152 adenoma size at any time after its generation. The growth function is based on a  
153 Janoschek growth curve and assumes that newly generated adenomas are 1 mm in  
154 size and can grow to a maximum of 50 mm.<sup>6,10</sup> Adenomas are not allowed to regress in  
155 size, although some grow very slowly, and most of which will never transition to CRC.

156 *Transition from adenoma to preclinical CRC*

157 CRC-AIM uses the log-normal function from CRC-SPIN v1.0 that allows  
158 adenomas to transition to preclinical cancer.<sup>10</sup> This function describes the cumulative  
159 transition probability of an adenoma transitioning to preclinical cancer at or before  
160 adenoma size ( $s$ ) is a function of the adenoma size, age at adenoma initiation ( $a$ ), sex  
161 (male vs female), and the location of the adenoma (colon vs rectum), and is defined as:

$$\xi_c(s, a) = \Phi\left(\frac{\{\ln(\gamma_{1cm}s) + \gamma_{2cm}(a - 50)\}}{\gamma_3}\right)$$

162 where  $\Phi$  is a standard normal cumulative distribution function (CDF). There are  
163 separate parameters based on adenoma location and sex: colon-male ( $cm$ ), colon-  
164 female ( $cf$ ), rectum-male ( $rm$ ), and rectum-female ( $rf$ ).

165 CRC-AIM uses a traditional cycle-based approach to aid in interpretability,  
166 whereas CRC-SPIN is a continuous time model.<sup>10</sup> We calculate adenoma size at the  
167 start of an interval, the size at the end of an interval ( $t+1$ ), and determine the probability  
168 of transitioning to CRC within the interval conditioned on the probability of having not yet  
169 transitioned by the adenoma size at time  $t$ , defined as:

$$\frac{\xi_c(s_{t+1}) - \xi_c(s_t)}{1 - \xi_c(s_t)}$$

170 *Preclinical cancer initiation*

171       When an adenoma transitions to preclinical CRC, multiple events in the model  
172 are triggered:

173       • Similar to CRC-SPIN, CRC-AIM assigns the preclinical CRC an initial size of 0.5  
174 mm and assumes that all CRCs grow exponentially within an adenoma until they  
175 overtake the adenoma. As a result, all CRCs are hypothetically detectable, since  
176 the minimum adenoma size is 1 mm and colonoscopy can detect 1 mm lesions.  
177 (Lesions are defined as the maximum of the adenoma and CRC sizes).<sup>10</sup>

178       • The sojourn time (ST) is determined.

179       • Independent of ST, the size of the preclinical cancer upon reaching ST is  
180 determined.

181       • The ST and the initial/final cancer sizes are used to enable the calculation of  
182 cancer size at any time.

183       • Cancer stage at diagnosis is determined based on cancer size upon reaching  
184 ST.

185 *Transition to clinically detectable CRC*

186       ST is modeled for the  $i$ -th individual's  $j$ -th preclinical cancer using a lognormal  
187 distribution that is conditional on location (colon versus rectum), similar to CRC-SPIN.<sup>10</sup>

188 *CRC size at clinical detection*

189       Similar to CRC-SPIN, when an adenoma transitions to preclinical CRC, CRC-  
190 AIM samples CRC size upon reaching ST.<sup>10</sup> The distribution of CRC sizes is based on  
191 Surveillance, Epidemiology, and End Results Program (SEER) data from 1975-1979

192 (prior to widespread CRC screening).<sup>10</sup> However, CRC-SPIN does not describe the form  
193 or parameterization of the smoothed distribution for size sampling.

194 CRC-AIM implements CRC size ( $s$ ) at clinical detection as a generalized log  
195 distribution, parameterized by location ( $\mu$ ), scale ( $\sigma$ ), and shape ( $\lambda$ ), with a maximum  
196 CRC size of 140 mm (see **Supplemental Material**). The probability density function is  
197 defined as:

$$\Phi \left\{ \frac{1}{\sigma} \left[ \log \left( \frac{s + \sqrt{s^2 + \lambda^2}}{2} \right) - \mu \right] \right\} \frac{s + \sqrt{s^2 + \lambda^2}}{\sigma (s^2 + \lambda^2 + s\sqrt{s^2 + \lambda^2})}$$

198 *CRC growth*

199 During the preclinical CRC phase, CRC-AIM assigns the cancer an initial size of  
200 0.5 mm. We replicated the methodology of CRC-SPIN that describes “flat spots” in the  
201 adenoma growth trajectory upon CRC initiation,<sup>10</sup> which we interpret to mean that upon  
202 initiation of a preclinical cancer, the preclinical cancer’s originating adenoma stops  
203 growing. We define “lesion size” as the larger value between adenoma size and  
204 preclinical cancer size.

205 Similar to CRC-SPIN, preclinical cancer follows an exponential growth curve in  
206 CRC-AIM, with size at time  $t$  from CRC initiation described as:

$$f(t) = ab^t$$

207 where  $a$  is the initial CRC size.

208 If we express initial CRC size as  $s_i$ , since the initial ( $s_i$ ) and final CRC size ( $s_f$ ) is  
209 known, and the time ( $t_{sf}$ ) required to reach the final CRC size is known (the  
210 independently sampled ST), then the rate ( $b$ ) can be calculated as:

$$b = \left( \frac{s_f}{s_i} \right)^{\frac{1}{t_{sf}}}$$

211 *CRC stage upon detection*

212 In CRC-AIM's natural history process, CRC is detected upon reaching ST and  
213 the presentation of disease signs and symptoms. (CRC can also be detected in the  
214 preclinical cancer growth phase, ie, during ST, during screening)

215 When CRC is detected, the American Joint Committee on Cancer (AJCC) CRC  
216 stage is determined based on its size. Similar to CRC-SPIN v1.0, we derived a  
217 multinomial logistic regression model fit to SEER 1975-1979 data to determine AJCC  
218 stage based on size (see **Supplemental Materials**). However, the actual form and  
219 parameterization of the multinomial logistic regression model used in CRC-SPIN v1.0 is  
220 not described. CRC-AIM uses the approach described below.

221 If we denote CRC size in millimeters as  $s$  in the  $i$ -th individual,  $k$  stage where  
222  $k=1, \dots, 4$ , then the logit ( $g$ ) for the  $i$ th individual for the  $k$ -th category, for categories  $k=1,$   
223  $2, \dots, K-1$ , is:

$$g_{ik} = \alpha_k + \beta_k s_i^{-0.5} + \gamma_k s_i$$

224 The probability of the  $i$ -th individual belonging to  $k$ -th category for categories  
225  $k=1, \dots, K$  is:

$$\pi_{ik} = \frac{\exp(g_{ik})}{\sum_{m=1}^K \exp(g_{im})}$$

226 where  $g_{iK} = 0$ .

227 For each individual  $i$ , the sum of the  $k$  probabilities adds to 1 and the cumulative  
228 probability across increasing stages (ie,  $\pi_{i1}, \pi_{i1} + \pi_{i2}, \pi_{i1} + \pi_{i2} + \pi_{i3}$ ) serve as thresholds  
229 to define CRC stage based on a uniform (0,1) CDF lookup. If an individual's CRC is  
230 identified prior to clinical diagnosis, its size would be smaller, the thresholds would shift,

231 and the sampled uniform (0,1) particular to that CRC would more likely yield an earlier  
232 CRC stage.

### 233 *CRC survival*

234 CRC-AIM implements cause-specific survival as a set of parametric regression  
235 equations that model survival probabilities, stratified by location and AJCC CRC stage,  
236 as a function of sex and age at diagnosis. To compare the survival outcomes of CRC-  
237 AIM to those of the CISNET models, we generated survival curves that mimicked the  
238 timeframes of SEER data used by CISNET both before and after their survival update in  
239 2013 (1975-1979 and 2000-2003, respectively). We used code developed by Deborah  
240 Schrag to convert pre-1988 SEER registry data from SEER historic staging criteria to  
241 AJCC staging categories<sup>13</sup>

242 We fit five separate parametric linear regression models for each AJCC stage  
243 and location (colon versus rectum), based on different distributions to describe survival  
244 time: Weibull, lognormal, exponential, Fréchet, and loglogistic (see **Supplemental**  
245 **Materials**). Model effects were sex and age at CRC diagnosis. We based model  
246 selection on the smallest Akaike information criterion (AICc) value for the fitted  
247 distribution across the five models for each AJCC stage and location (**Table S1**). CRC-  
248 AIM uses the CDFs described by the selected model to determine the age at CRC-  
249 specific death as a function of age at diagnosis and/or sex. The regression-based  
250 coefficients are multiplied by an indicator function if sex or age at diagnosis criteria are  
251 met (sex indicator is 1 if met, -1 if not met; age at diagnosis indicator is 1 if met, 0 if not  
252 met).

253

## 254 Screening Overlay

255           The screening component of CRC-AIM is derived from basic assumptions about  
256 CRC screening. In general, CRC screening facilitates the detection and removal of  
257 adenomas and preclinical lesions. Each time screening is due, the chance of a lesion to  
258 be detected is dependent on the screening test's sensitivity and reach. The overall  
259 effectiveness of screening is dependent on screening frequency, adherence rates, and  
260 the sensitivity and specificity of the screening test. False positives can occur in relation  
261 to a screening test's specificity and lead to unnecessary follow-up colonoscopies or  
262 unnecessary polypectomies. Complications, including fatal ones, can arise due to  
263 polypectomies. Thus, adverse events related to colonoscopies are part of the screening  
264 component.

265           For the purposes of this analysis, the screening test characteristic input  
266 assumptions were the same as those used in CISNET models (**Table 2**),<sup>2,14</sup> which we  
267 have reproduced here in greater detail. We assumed that the same test characteristics  
268 for screening colonoscopies applied to colonoscopies for diagnostic follow-up or for  
269 surveillance, and that there was no correlation in findings between CTC or  
270 sigmoidoscopy and subsequent diagnostic colonoscopy. For colonoscopy and  
271 sigmoidoscopy, the lack of specificity with endoscopy reflects the detection of  
272 nonadenomatous polyps. For sigmoidoscopy, this may lead to an unnecessary  
273 diagnostic colonoscopy, and for colonoscopy, this may lead to an unnecessary  
274 polypectomy. For computed tomographic colonography, the lack of specificity reflects  
275 the detection of  $\geq 6$  mm nonadenomatous lesions, artifacts, stool, and adenomas smaller  
276 than the 6-mm threshold for referral to colonoscopy that are measured as  $\geq 6$  mm. For

277 FIT, we assumed a positivity cutoff of  $\geq 100$  ng of hemoglobin (Hb) per mL of buffer ( $\geq 20$   
278 mcg Hb/g of feces). For FIT and mt-sDNA, the sensitivity for adenomas  $< 10$  mm was  
279 considered the sensitivity for nonadvanced adenomas. For the high sensitivity guaiac  
280 based fecal occult blood test (HSgFOBT), we assumed that 1-5 mm adenomas do not  
281 bleed and therefore cannot cause a positive stool test. It was also assumed that  
282 HSgFOBT can be positive because of bleeding from other causes, the probability of  
283 which is equal to positivity rate in individuals without adenomas.

284 The sensitivity inputs for stool-based tests are per person and are based on the  
285 characteristics of the most advanced lesion. The sensitivity inputs for structural tests are  
286 per lesion and potential detection of lesions depend on the reach of the test. It is  
287 assumed that sigmoidoscopy completely visualizes the rectum for all individuals,  
288 visualizes the sigmoid colon in 88% of individuals, and visualizes the descending colon  
289 in 6% of individuals.<sup>3,15,16</sup> With colonoscopy, full reach (to the cecum) is assumed to be  
290 achieved 95% of the time and if reach is only partial, a second colonoscopy is  
291 performed.<sup>2</sup>

292 It is assumed that a follow-up colonoscopy occurs after any positive non-  
293 colonoscopy screening test. If the follow-up colonoscopy is negative, individuals return  
294 to their original non-colonoscopy screening test and the next screening is due in 10  
295 years. If the follow-up colonoscopy is positive for an adenoma of any size, individuals  
296 enter a surveillance colonoscopy period where the next colonoscopy is based on the  
297 findings of the latest colonoscopy (3 years if a detected adenoma is  $\geq 10$  mm or if  $\geq 3$   
298 adenomas of any size are detected; 5 years if 1-2 adenomas  $< 10$  mm are detected;  
299 these are the same histology assumptions used by CISNET). Surveillance continues

300 until at least age 85 and then halts if no adenomas or CRC are detected on the last  
301 surveillance exam or continues past 85 until no adenomas or CRC are detected on a  
302 surveillance exam. Individuals with preclinical lesions that become symptomatic based  
303 on sojourn time expiration receive a colonoscopy to clinically diagnose interval cancers  
304 (CRCs that grow and develop after a screening or surveillance exam but before the next  
305 recommended exam).

306 Three types of complications related to colonoscopies are included in the model:

307 1) serious gastrointestinal events (e.g., perforations, gastrointestinal bleeding, or  
308 transfusions) of which 8.97% were perforations<sup>17</sup> and 5.19% of perforations led to  
309 death<sup>18</sup>; 2) other gastrointestinal events (e.g., paralytic ileus, nausea and vomiting,  
310 dehydration, abdominal pain); and 3) cardiovascular events (e.g., myocardial infarction  
311 or angina, arrhythmia, congestive heart failure, cardiac or respiratory arrest, syncope,  
312 hypotension, or shock). Risk of complications increases by age.<sup>17,18</sup> (For additional  
313 information, see eFigure1 of Knudsen et al.<sup>2</sup>) Because the risk of complications with  
314 colonoscopy is conditional on polypectomy,<sup>17,19</sup> and sigmoidoscopy is modeled without  
315 a biopsy or polypectomy of detected lesions, the risk of complications with  
316 sigmoidoscopy was therefore assumed to be none.

317 The screening modalities evaluated for the main validation analysis were FIT,  
318 HSgFOBT, mt-sDNA, and colonoscopy.

319

### 320 CRC-AIM Comparison and Cross-Validation

321 To evaluate the performance of CRC-AIM, we compared the outputs of CRC-AIM  
322 against the natural history experiment outputs of CRC-SPIN, SimCRC, and MISCAN.



323 We compared the CRC-AIM natural history outputs to those from CRC-SPIN v1.0, as  
324 well as the other CISNET models' outputs, that were generated prior to 2013 and the  
325 associated CISNET CRC survival update. For comparisons to these historical (pre-  
326 2013) outputs, we selected the 1975-1979 time period for CRC cause-specific survival  
327 curves, because this time period had been described as previously used by CRC-  
328 SPIN.<sup>10</sup> We also compared the outputs from CRC-AIM to natural history outputs  
329 presented in the 2015 CISNET technical report.<sup>14</sup> For these comparisons, we used the  
330 2000-2003 time period for CRC cause-specific survival curves, similar to what CISNET  
331 used for recently diagnosed CRC.<sup>20</sup>

332 All CRC-AIM analyses use cohort life tables for non-CRC mortality unless  
333 otherwise specified. We attempted to match birth cohorts to those from the original  
334 CISNET analyses, but this information was not always reported. Data from reference  
335 publications<sup>12,14,21,22</sup> were extracted using a custom Python package that assigns  
336 numeric values based on the pixel location of data within a figure and the corresponding  
337 X and Y scale values.

#### 338 *Comparison to historic (pre-2013) outputs*

339 Adenoma and CRC Prevalence/Incidence: We compared the adenoma and CRC  
340 prevalence/incidence values for individuals at the age of 65, as described by Knudsen  
341 et al.<sup>21</sup> Results were reported either as a rate per thousand individuals or by  
342 percentage. Because the cost-basis year used by Knudsen et al was 2007,<sup>21</sup> and we  
343 wanted to replicate their simulation of 65-year-olds, we assumed a birth cohort of 1942  
344 (2007 minus 65). The number of simulated individuals was not reported but we  
345 assumed 3 million. Furthermore, we excluded individuals with existing preclinical cancer

346 at age 65 from the CRC cumulative incidence calculations under the assumption that  
347 CRC incidence measures clinically diagnosed CRC. In addition, we compared the  
348 multiplicity of adenomas (the average number of adenomas in individuals with one or  
349 more adenomas), as described in Kuntz et al.<sup>12</sup>

350 Adenoma Dwell Time, Sojourn Time (ST), and Overall Dwell Time: We replicated  
351 the retrospective analysis from Kuntz et al<sup>12</sup> that calculated the mean, median, and  
352 interquartile range (IQR) for adenoma dwell time, the ST, and the overall dwell time  
353 (adenoma dwell time plus ST) for individuals with clinically diagnosed CRC. We  
354 simulated a cohort of 30 million individuals born in 1944. We also compared CRC-AIM's  
355 outputs to different mean values of these characteristics as reported one year earlier by  
356 CRC-SPIN,<sup>22</sup> although the birth cohort for that analysis was different (CRC-SPIN had  
357 simulated 30 million individuals born in 1928).

358 Estimated Annual Transition Probabilities: We replicated a modeling experiment  
359 estimating transition probabilities from Rutter and Savarino.<sup>22</sup> We simulated 30 million  
360 individuals born in 1928 and estimated state-transition probabilities for a cohort of 60-  
361 year-olds, which are based on the proportion of individuals making state transitions as  
362 they progress from age 60 to 61.

### 363 *Comparison to USPSTF outputs*

#### 364 *Natural History Comparison*

365 We compared the natural history outputs from CRC-AIM to those described in  
366 the 2015 CISNET technical report by Zauber et al.<sup>14</sup> For each comparison, we  
367 replicated the reference population by simulating 2 million individuals using a birth  
368 cohort year of 1975.

369           Prevalence of Preclinical CRC/Adenomas: We replicated the outputs describing  
370 the prevalence of preclinical CRC and adenomas for individuals over 40 years old. In  
371 our calculation of preclinical cancer prevalence, once an individual developed clinically  
372 detectable cancer, they no longer had preclinical cancer and were removed from the  
373 numerator. Therefore, this analysis does not represent the cumulative probability of  
374 acquiring preclinical cancer by a certain age. In our calculation of adenoma prevalence,  
375 we only considered adenomas that were present until clinical CRC developed.

376           Location/Size of Adenomas: We replicated the location and size of adenomas for  
377 individuals over 40 years old. For the size analysis, only the size of the most advanced  
378 adenoma (ie, largest lesion) was considered for the adenoma distribution. Again,  
379 adenomas were only included until clinical CRC developed.

380           CRC Incidence by Age: We replicated the incidence of clinically diagnosed CRC  
381 cases per 100,000 individuals by age, which was calibrated to 1975-1979 SEER  
382 incidence (without screening). This incidence was compared to the empirical SEER  
383 incidence rates prior to the diffusion of screening (1975-1979) and after over half of the  
384 population had been screened (2007-2011). We calculated the incidence of new  
385 clinically diagnosed CRC that occurred between yearly intervals, starting at 2015-2016  
386 (age 40) and projected through 2075-2076 (age 100). Individuals with clinically  
387 diagnosed CRC for a given interval were excluded for future intervals.

388           CRC Stage Distribution at Diagnosis: We generated a stage distribution of  
389 clinically diagnosed CRC in individuals aged 40 and older in the absence of screening.

390           Cumulative Probability of Developing/Dying from CRC: We determined the  
391 cumulative probability of developing CRC and dying from CRC, by age, in the absence

392 of screening using a birth year of 1975. This was performed using both cohort life  
393 tables, described in detail above, and period life tables, which were obtained from the  
394 Centers for Disease Control and Prevention.<sup>8</sup>

395 Cumulative Probability of Developing CRC in Individuals with/without Underlying  
396 Lesions: We replicated an experiment by Kuntz et al<sup>12</sup> that determined the cumulative  
397 probability of developing CRC, stratified by individuals who either did or did not have an  
398 existing adenoma or undiagnosed preclinical cancer at age 55. The analysis extended  
399 to age 85. The weighted average of the two groups reflects the population-level risk of  
400 cumulative CRC incidence across age. Competing cause of mortality (ie, death from  
401 other causes) was removed, and the cumulative probability of developing CRC in this  
402 analysis was therefore not impacted by choice of life table.

#### 403 *Screening Outcomes*

404 We replicated the screening outcomes supplemental tables from the CISNET  
405 technical report for each screening modality.<sup>14</sup> We wanted to reproduce CISNET model  
406 outputs as faithfully as possible, and therefore we used the modified CRC-AIM that  
407 employs period life tables. Predicted screening outcomes were simulated for a birth  
408 year cohort of 1975. The main benefits of CRC screening are life-years gained (LYG)  
409 from prevention of CRC cases and delay of CRC deaths compared with no screening.  
410 Number of colonoscopies was used to represent burden and harms. The number of  
411 tests, complications from colonoscopies, CRC cases, CRC deaths, life-years with CRC,  
412 incidence reduction, and mortality reduction were additional screening outcomes. All  
413 outcomes were reported per 1,000 individuals free of diagnosed CRC at age 40.

414           Efficient Frontiers: We replicated the efficient frontier figures from the Figure 3  
415 (colonoscopy) and Figure 4 (stool-based—FIT, HSgFOBT, and mt-sDNA) and  
416 corresponding tables from Knudsen et al.<sup>2</sup> Like CISNET, for both colonoscopy and  
417 stool-based efficient frontiers, the screening stop ages were 75, 80, or 85 years. We  
418 included only screening start ages of 50 and 55 for colonoscopy and replicated the  
419 screening start ages of 50 and 55 for stool-based modalities. Strongly dominated  
420 strategies (ie, strategies that colonoscopies for fewer LYG) were discarded. The  
421 incremental number of LYG per 1000 ( $\Delta$ LYG) and incremental number of colonoscopies  
422 per 1000 ( $\Delta$ COL) were computed. The efficiency ratio ( $\Delta$ COL/ $\Delta$ LYG) for each remaining  
423 strategy was calculated. Strategies with fewer LYG but a higher efficiency ratio than  
424 another strategy were discarded as weakly dominated. The efficient frontier was the line  
425 that connected the efficient strategies; strategies that had LYG within 98% of the  
426 efficient frontier were considered near-efficient.

#### 427 *Cross-validation of screening outcomes*

428           The purposes of the validation analysis were to cross-validate CRC-AIM's  
429 screening component with other CISNET screening comparative effectiveness results  
430 assuming perfect adherence. Colonoscopy and stool CISNET screening modalities  
431 were analyzed in the validation analysis. For more information on the comparative  
432 analyses, see **Supplemental Materials**.

433

## 434 **Results**

435 We compared the natural history outputs from CRC-AIM with the published  
436 outputs from the three CISNET models—CRC-SPIN, SimCRC, and MISCAN—and  
437 found considerable similarity among the models.

438 First, CRC-AIM produced similar natural history outputs compared to CRC-SPIN  
439 v1.0, SimCRC, and MISCAN prior to the 2013 CISNET CRC survival update. The  
440 adenoma prevalence at age 65 for CRC-AIM is 29.2%, which is similar to the CISNET  
441 models (30.7% for CRC-SPIN, 37.2% for SimCRC, and 39.8% for MISCAN) (**Table 1**).  
442 Moreover, the multiplicity of adenomas at age 65 for CRC-AIM (1.7) was within the  
443 range of values for the CISNET models (1.8 for CRC-SPIN, 1.6 for SimCRC, and 2.0 for  
444 MISCAN) (**Table 1**). In addition, the location (proximal colon, distal colon, and rectum)  
445 of the number of size-stratified adenomas (1-5 mm, 6-9 mm, and  $\geq 10$  mm), along with  
446 the cumulative incidence (10-year, 20-year, and lifetime) across CRC stages, was  
447 comparable between CRC-AIM and the CISNET models (**Figure 2, Table 1**).

448 There was a comparable percentage of CRCs among CRC-AIM, CRC-SPIN, and  
449 SimCRC that developed from adenomas generated within 10 and 20 years of the  
450 clinical CRC diagnosis (**Figure S1, Table 2**). Although CRC-AIM's overall dwell time is  
451 longer than the ranges reported for CRC-SPIN and SimCRC by Kuntz et al,<sup>12</sup> it is less  
452 than another published estimate for CRC-SPIN<sup>22</sup> (**Figure 3, Table S2**). CRC-AIM's  
453 derived annual transition probabilities align closely with those of CRC-SPIN (**Table S3**),  
454 except for preclinical CRC transition probabilities.

455 Second, we observed consistent natural history outputs between CRC-AIM and  
456 the CISNET-based outputs described in the CISNET CRC technical report.<sup>14</sup> The  
457 prevalence of preclinical CRC estimated by CRC-AIM is within the range of the CISNET

458 models (**Figure 4A**). Because preclinical cancer prevalence is sensitive to sojourn  
459 time,<sup>14</sup> if CRC-AIM used the original sojourn time parameter estimates from CRC-  
460 SPIN,<sup>7</sup> then CRC-AIM's prevalence would align with the prevalence reported by Berg et  
461 al<sup>23</sup> (see **Supplemental Material**).

462 CRC-AIM's adenoma prevalence almost overlaps that of CRC-SPIN (**Figure 4B**,  
463 **Table S4**). Both CRC-AIM and CRC-SPIN estimate lower adenoma prevalence  
464 compared to SimCRC and MISCAN, until approximately age 80 (**Figure 4B**, **Table S4**).  
465 The CRC-AIM CRC incidence curve overlaps the three CISNET models and 1975-1979  
466 SEER estimates, trending more closely with CRC-SPIN than SimCRC or MISCAN after  
467 age 85 (**Figure 4C**). The distribution of adenoma location in CRC-AIM is identical to that  
468 of CRC-SPIN (**Figure S2**), and the distribution of adenomas by size of the most  
469 advanced adenoma among individuals aged 40, 60, and 80 is similar to CRC-SPIN  
470 (**Figure 5**). The CRC-AIM cancer stage distribution is almost identical to CRC-SPIN,  
471 with both models producing lower Stage IV cancer estimates compared to SimCRC and  
472 MISCAN due to a similar method to assign cancer stage probability<sup>1</sup> (**Figure 6**).

473 Additionally, we used CRC-AIM to explore the sensitivity of natural history  
474 modeling outputs (cumulative probability of developing CRC, cumulative risk of dying  
475 from CRC, and life expectancy) in an unscreened population based on the choice of life  
476 tables (cohort versus period; see **Methods** for details) for non-CRC-related mortality.  
477 CRC-AIM uses cohort life tables, which are preferred over period life tables for  
478 predicting future mortality.<sup>8,9</sup> Although the CISNET models use period life tables,  
479 multiple natural history outputs between CRC-AIM and the CISNET models are  
480 generally comparable, with the exceptions of cumulative CRC risk and CRC mortality.

481           The curves describing the cumulative probability of developing CRC between  
482 ages 40 and 100 are similar between default CRC-AIM (with cohort life tables) and the  
483 CISNET models until age 80, after which CRC-AIM estimates more CRC (**Figure 7**).  
484 The cumulative probability is 8.0% for default CRC-AIM compared to 7.2% for CRC-  
485 SPIN, 7.0% for SimCRC, and 6.7% for MISCAN. Using period life tables, CRC-AIM  
486 generates an overlapping probability curve and a comparable cumulative probability of  
487 7.1% (**Figure 7**). Similarly, the cumulative probability curve of dying from CRC between  
488 ages 40 and 100 is nearly identical to the CISNET models until age 80, after which  
489 CRC-AIM estimates more CRC deaths (**Figure 7**). The cumulative probability of dying  
490 from CRC is 3.2% in CRC-AIM using period tables and 3.7% in CRC-AIM using cohort  
491 tables, compared to 2.7% for CRC-SPIN and 2.8% for SimCRC and MISCAN.<sup>14</sup>For life  
492 expectancy, we replicated the CISNET model analysis by using period tables and  
493 assuming a simulation stop-age of 100 years. The life expectancy among 40-year-olds  
494 was 39.63 years for the modified CRC-AIM, which was almost identical to the CISNET  
495 models (39.6 years for SimCRC, 40.0 years for both MISCAN and CRC-SPIN). All three  
496 CISNET models simulate out to 100 years due to the unreliability of period life table  
497 estimates after age 100. Using the default cohort life tables, CRC-AIM simulated a life  
498 expectancy among 40-year-olds of 41.1 years, assuming a stop-age of 100 years.  
499 Because cohort life tables allow for the simulation of stop-ages beyond 100 years, we  
500 evaluated the simulated life expectancy for CRC-AIM given an assumed stop-age of  
501 120 years, which was 41.7 years.

502           Finally, we replicated the analysis from Kuntz et al<sup>12</sup> where cumulative probability  
503 of developing CRC was considered purely as a function of the adenoma-carcinoma



504 sequence and the competing risk of mortality is eliminated (ie, removing life tables from  
505 consideration). For the 20-year cumulative CRC incidence (at age 75) for individuals  
506 with underlying lesions and without competing mortality, CRC-AIM projected 13.5%,  
507 which is comparable to the CISNET models (13.5% for CRC-SPIN, 13.1% for SimCRC,  
508 and 8.6% for MISCAN) (**Figure 8**). Similar results were obtained for the risk ratios at  
509 age 75 for the group of individuals with lesions (at age 55) compared to the group  
510 without underlying lesions (at age 55)—CRC-AIM projected a risk ratio of 37.3, within  
511 the range of the CISNET models (75 for CRC-SPIN, 29 for SimCRC, and 7 for  
512 MISCAN) (**Figure 8**).

513         The screening overlay validation analysis assumed perfect adherence for CRC  
514 screening strategies. We generated screening overlay tables from CISNET publication  
515 (**Tables S36-43**) using CRC-AIM with period life tables. When no screening was  
516 conducted, the CRC-AIM model estimated that 71.1 out of 1000 individuals free of CRC  
517 at age 40 would be diagnosed with CRC during their lifetime and 31.7 would die of CRC  
518 (**Table S36**). When screening was conducted, all strategies provided clinical benefit in  
519 terms of LYG and reductions in CRC-related incidence and mortality (**Tables S36-43**).  
520 With those tables, we were able to compute the efficient frontiers (**Figure 9** and **Tables**  
521 **S44-45**).

522         We conducted three analyses to demonstrate model cross-validation (1)  
523 quantitative method comparison, in which screen-related outcomes from all models  
524 were compared, using Passing-Bablok regression, in terms of systemic bias,  
525 proportional bias, and total bias at the low and high measurement range; (2) qualitative  
526 efficient frontier comparison, in which the efficient frontiers from all models were

527 compared using concordance analysis; (3) medical decision making comparison, in  
528 which the final recommended screening strategies from all models were compared (see  
529 **Supplemental Material**).

530 Overall, there is substantial overlap across multiple natural history and screening  
531 overlay outputs between CRC-AIM and the CISNET models, especially CRC-SPIN.

532

### 533 **Discussion**

534 We developed a robust natural history model of colorectal cancer—the Colorectal  
535 Cancer and Adenoma Incidence & Mortality (CRC-AIM) microsimulation model—to  
536 facilitate greater opportunities and efficiencies in collaborative modeling research. We  
537 compared the results of CRC-AIM with published results for the three CISNET CRC  
538 models: CRC-SPIN, SimCRC, and MISCAN.

539 The percentage of adenomas that had developed within 10 or 20 years prior to  
540 clinical CRC diagnosis is similar between CRC-AIM and the CISNET models (**Figure**  
541 **S1, Table 2**). This similarity suggests a comparable interaction between screening  
542 interval and CRC incidence reduction. If the adenoma transition rates are similar, then  
543 the screening benefits will be comparable because all models will have similar windows  
544 of opportunity for a hypothetical screen to detect and remove CRC-causing  
545 adenomas.<sup>12</sup> However, if there is a difference in the proportion of adenomas that  
546 become cancerous within a particular timeframe, then the models could have different  
547 reductions in CRC incidence and mortality, depending on the screening modality.<sup>12</sup>  
548 Because of this similarity, CRC-AIM demonstrated relative comparability with the

549 CISNET models in terms of CRC incidence and mortality reduction and conclusions  
550 related to medical decision making.

551 Although the natural history outputs from CRC-AIM generally aligned with the  
552 CISNET models, there were some notable differences. CRC-AIM's derived annual  
553 transition probabilities align closely with those of CRC-SPIN (**Table S3**), except for  
554 preclinical CRC transition probabilities, which is likely caused by specifying a different  
555 sojourn time (ST) for CRC-AIM (**Table S2**; see **Supplemental Material**). When the  
556 original CRC-SPIN parameter estimates are used for ST, the preclinical CRC transition  
557 probabilities are similar between CRC-AIM and CRC-SPIN (data not shown).

558 Minor differences in cumulative cancer mortality by age 100 (natural history) and  
559 life-years-gained (screening overlay) are likely due to a different method for calculating  
560 CRC survival between CRC-AIM (cause-specific survival) and the CISNET models  
561 (relative survival). The outcomes between relative survival and cause-specific survival  
562 are generally comparable; although relative survival is more commonly used with  
563 registry data, cause-specific survival benefits from enhanced flexibility and can better  
564 incorporate risk factors for particular populations.<sup>24,25</sup> Because the CISNET models use  
565 identical CRC-based survival functions,<sup>14,20,26,27</sup> the potential inter-model variability that  
566 would have occurred if each group had independently developed their own survival  
567 functions is unknown. Since CRC-AIM's cause-specific survival functions overlap  
568 considerably with the CISNET models until age 85, after which only minor deviations  
569 are observed, we predict that CRC-AIM's cumulative cancer mortality would lie within an  
570 inter-model variability.

571 In our analysis, we compared the impact of cohort versus period life tables on the  
572 sensitivity of natural history outputs in an unscreened population. CRC-AIM uses cohort  
573 life tables, which determine annual survival from past mortality rates and/or projected  
574 mortality rates. The CISNET models use period life tables, which describe what would  
575 happen to a hypothetical cohort if it experienced, throughout its entire life, the mortality  
576 conditions of a particular time period. In general, cohort tables are preferred over period  
577 life tables for predicting future mortality,<sup>8,9</sup> and the latter may underestimate survival  
578 because they only represent a snapshot of the current mortality experience.<sup>8,9</sup>

579 We demonstrate that the choice of life table impacts CRC incidence and  
580 mortality, particularly after age 85. The differences in cumulative probability of  
581 developing CRC after age 85 in CRC-AIM compared to the CISNET models is primarily  
582 driven by using cohort life tables—older individuals are alive and at risk of developing  
583 CRC. Consequently, this impacts cumulative mortality, because more individuals will die  
584 of CRC if more individuals develop CRC. We found that choice of life table did not  
585 significantly impact other modeling outputs.

586 In general, by conforming to CISNET's assumptions regarding their efficient  
587 frontier calculations, we reproduced their overall screening outputs (**Figure 9**). We also  
588 conducted multiple model cross-validation comparisons between CRC-AIM and the  
589 CISNET models. For comparisons based on quantitative outcomes, qualitative efficient  
590 frontiers, and overall strategy recommendations, we found that the differences in  
591 outcomes between CRC-AIM and the CISNET models were generally similar to the  
592 differences among the CISNET models themselves (see **Supplemental Materials**).  
593 Quantitative differences for CRC-AIM versus the CISNET models were observed with

594 total surveillance colonoscopies, total colonoscopies, and life-years-gained, depending  
595 on the comparison that was performed. Regardless, qualitative decisions related to  
596 inform clinical practice in terms of screening modality using CRC-AIM are almost  
597 identical to those made by the CISNET models. One limitation of our analyses is that  
598 were limited to the descriptions of model parameters and assumptions found in the  
599 CISNET model publications, which we replicated as closely as possible. These models  
600 have likely been altered over time and some analytical details are not provided within  
601 the publications.

602         With CRC-AIM, we want to stimulate community engagement and enhance  
603 research into underexplored questions in population health by clearly articulating its  
604 assumptions and framework. To that end, we have deposited CRC-AIM's formulas,  
605 parameters, and additional documentation on a publicly accessible repository  
606 (<https://github.com/CRCAIM/CRC-AIM-Public>). (This information is also included in  
607 **Table S5** and **Supplemental Material**.) In addition, we will make CRC-AIM's underlying  
608 Python code available to collaborators to facilitate information-sharing and emphasize  
609 visibility and transparency. We have included additional details regarding opportunities  
610 for collaboration on the CRC-AIM repository.

611 **Acknowledgments**

612 Medical writing and editorial/data visualization support were provided by David K  
613 Edwards V, PhD, with assistance from Rebecca Swartz, PhD (both of Exact Sciences,  
614 Madison, WI) and Erin P Scott, PhD (Maple Health Group, LLC; funded by Exact  
615 Sciences).

616 We would like to thank A Burak Ozbay, PhD (Exact Sciences) and Marcus  
617 Parton (Exact Sciences) for helpful guidance and overall feedback; David Young, MS  
618 (Auburn University) and Gennadiy Gorelik, PhD (EmpiriQA) for technical advice; and  
619 Evan Musick (Exact Sciences) for assistance with data visualization.

620

621 **Permissions**

622 Permissions will be obtained from the publishers as needed.

623

624 **Declaration of Conflicting Interests**

625 Financial support for this study was provided entirely by a contract with Exact  
626 Sciences Corporation. The funding agreement ensured the authors' independence in  
627 designing the model, interpreting the data, writing, and publishing the report. The  
628 following authors are employed by the sponsor: MM and LS.

629 AP has a consulting contract with the sponsor through EmpiriQA. HR has a  
630 consulting contract with the sponsor through BioBridge Strategies. AMF has a  
631 consulting contract with the sponsor. PJJ serves as Chief Medical Officer for Screening  
632 at Exact Sciences through a contracted services agreement with Mayo Clinic. PJJ and  
633 Mayo Clinic have contractual rights to receive royalties through this agreement.

634 KHL does not have a consulting contract with the sponsor. All other authors  
635 declare no conflicts of interest.

636 **References**

- 637 1. CISNET Colorectal Cancer Collaborators. Joint Profile (all profiles combined).  
638 HI.001.03122015.70057 <https://cisnet.cancer.gov/colorectal/profiles.html>.
- 639 2. Knudsen AB, Zauber AG, Rutter CM, et al. Estimation of Benefits, Burden, and  
640 Harms of Colorectal Cancer Screening Strategies: Modeling Study for the US  
641 Preventive Services Task Force. *JAMA*. 2016;315(23):2595-2609.
- 642 3. Rutter CM, Knudsen AB, Marsh TL, et al. Validation of Models Used to Inform  
643 Colorectal Cancer Screening Guidelines: Accuracy and Implications. *Med Decis*  
644 *Making*. 2016;36(5):604-614.
- 645 4. Zucchelli E, Jones AM, Rice N. The evaluation of health policies through dynamic  
646 microsimulation methods. *International Journal of Microsimulation*. 2012;5(1):2-  
647 20.
- 648 5. Rutter CM, Zaslavsky AM, Feuer EJ. Dynamic microsimulation models for health  
649 outcomes: a review. *Med Decis Making*. 2011;31(1):10-18.
- 650 6. CISNET Colorectal Cancer Collaborators. RAND Corporation (CRC-SPIN), 2018.  
651 HI.001.11302018.9737:<https://cisnet.cancer.gov/colorectal/profiles.html>.
- 652 7. Rutter CM, Miglioretti DL, Savarino JE. Bayesian Calibration of Microsimulation  
653 Models. *J Am Stat Assoc*. 2009;104(488):1338-1350.
- 654 8. Arias E. United States life tables, 2010. *Natl Vital Stat Rep*. 2014;63(7):1-63.
- 655 9. Bell FC, Miller ML. Life Tables for the United States Social Security Area 1900-  
656 2100. 2005; [https://www.ssa.gov/oact/NOTES/pdf\\_studies/study120.pdf](https://www.ssa.gov/oact/NOTES/pdf_studies/study120.pdf).
- 657 10. CISNET Colorectal Cancer Collaborators. RAND Corporation (CRC-SPIN), 2015.  
658 HI.001.03112015.70373:<https://cisnet.cancer.gov/colorectal/profiles.html>.



- 659 11. Statistical Abstract Series. U.S. Census Bureau.  
660 [https://www.census.gov/library/publications/time-series/statistical\\_abstracts.html](https://www.census.gov/library/publications/time-series/statistical_abstracts.html).
- 661 12. Kuntz KM, Lansdorp-Vogelaar I, Rutter CM, et al. A systematic comparison of  
662 microsimulation models of colorectal cancer: the role of assumptions about  
663 adenoma progression. *Med Decis Making*. 2011;31(4):530-539.
- 664 13. Schrag D. AJCC Staging: Staging Colon Cancer Patients using the TNM system  
665 from 1975 to the present. 2007;  
666 [https://www.mskcc.org/departments/epidemiology-](https://www.mskcc.org/departments/epidemiology-biostatistics/epidemiology/ajcc-staging)  
667 [biostatistics/epidemiology/ajcc-staging](https://www.mskcc.org/departments/epidemiology-biostatistics/epidemiology/ajcc-staging).
- 668 14. Zauber A, Knudsen AB, Rutter CM, Lansdorp-Vogelaar I, Kuntz KM. Technical  
669 Report: Evaluating the benefits and harms of colorectal cancer screening  
670 strategies: a collaborative modeling approach. 2015; AHRQ Publication No. 14-  
671 05203-EF-  
672 2:[https://www.uspreventiveservicestaskforce.org/Home/GetFile/1/16540/cisnet-](https://www.uspreventiveservicestaskforce.org/Home/GetFile/1/16540/cisnet-draft-modeling-report/pdf)  
673 [draft-modeling-report/pdf](https://www.uspreventiveservicestaskforce.org/Home/GetFile/1/16540/cisnet-draft-modeling-report/pdf).
- 674 15. Atkin WS, Cook CF, Cuzick J, et al. Single flexible sigmoidoscopy screening to  
675 prevent colorectal cancer: baseline findings of a UK multicentre randomised trial.  
676 *Lancet*. 2002;359(9314):1291-1300.
- 677 16. Painter J, Saunders DB, Bell GD, Williams CB, Pitt R, Bladen J. Depth of  
678 insertion at flexible sigmoidoscopy: implications for colorectal cancer screening  
679 and instrument design. *Endoscopy*. 1999;31(3):227-231.

- 680 17. Warren JL, Klabunde CN, Mariotto AB, et al. Adverse events after outpatient  
681 colonoscopy in the Medicare population. *Ann Intern Med.* 2009;150(12):849-857,  
682 W152.
- 683 18. Gatto NM, Frucht H, Sundararajan V, Jacobson JS, Grann VR, Neugut AI. Risk  
684 of perforation after colonoscopy and sigmoidoscopy: a population-based study. *J*  
685 *Natl Cancer Inst.* 2003;95(3):230-236.
- 686 19. van Hees F, Zauber AG, Klabunde CN, Goede SL, Lansdorp-Vogelaar I, van  
687 Ballegooijen M. The appropriateness of more intensive colonoscopy screening  
688 than recommended in Medicare beneficiaries: a modeling study. *JAMA Intern*  
689 *Med.* 2014;174(10):1568-1576.
- 690 20. Rutter CM, Johnson EA, Feuer EJ, Knudsen AB, Kuntz KM, Schrag D. Secular  
691 trends in colon and rectal cancer relative survival. *J Natl Cancer Inst.*  
692 2013;105(23):1806-1813.
- 693 21. Knudsen AB, Lansdorp-Vogelaar I, Rutter CM, et al. Cost-effectiveness of  
694 computed tomographic colonography screening for colorectal cancer in the  
695 medicare population. *J Natl Cancer Inst.* 2010;102(16):1238-1252.
- 696 22. Rutter CM, Savarino JE. An evidence-based microsimulation model for colorectal  
697 cancer: validation and application. *Cancer Epidemiol Biomarkers Prev.*  
698 2010;19(8):1992-2002.
- 699 23. Berg JW, Downing A, Lukes RJ. Prevalence of undiagnosed cancer of the large  
700 bowel found at autopsy in different races. *Cancer.* 1970;25(5):1076-1080.

- 701 24. Howlader N, Ries LA, Mariotto AB, Reichman ME, Ruhl J, Cronin KA. Improved  
702 estimates of cancer-specific survival rates from population-based data. *J Natl*  
703 *Cancer Inst.* 2010;102(20):1584-1598.
- 704 25. Forjaz de Lacerda G, Howlader N, Mariotto AB. Differences in Cancer Survival  
705 with Relative versus Cause-Specific Approaches: An Update Using More  
706 Accurate Life Tables. *Cancer Epidemiol Biomarkers Prev.* 2019;28(9):1544-1551.
- 707 26. van der Steen A, Knudsen AB, van Hees F, et al. Optimal colorectal cancer  
708 screening in states' low-income, uninsured populations-the case of South  
709 Carolina. *Health Serv Res.* 2015;50(3):768-789.
- 710 27. Meester RG, Zauber AG, Doubeni CA, et al. Consequences of Increasing Time  
711 to Colonoscopy Examination After Positive Result From Fecal Colorectal Cancer  
712 Screening Test. *Clin Gastroenterol Hepatol.* 2016;14(10):1445-1451 e1448.
- 713 28. Schroy PC, 3rd, Coe A, Chen CA, O'Brien MJ, Heeren TC. Prevalence of  
714 advanced colorectal neoplasia in white and black patients undergoing screening  
715 colonoscopy in a safety-net hospital. *Ann Intern Med.* 2013;159(1):13-20.
- 716 29. van Rijn JC, Reitsma JB, Stoker J, Bossuyt PM, van Deventer SJ, Dekker E.  
717 Polyp miss rate determined by tandem colonoscopy: a systematic review. *Am J*  
718 *Gastroenterol.* 2006;101(2):343-350.
- 719 30. Imperiale TF, Ransohoff DF, Itzkowitz SH, et al. Multitarget stool DNA testing for  
720 colorectal-cancer screening. *N Engl J Med.* 2014;370(14):1287-1297.
- 721 31. Lin JS, Piper MA, Perdue LA, et al. U.S. Preventive Services Task Force  
722 Evidence Syntheses, formerly Systematic Evidence Reviews. In: *Screening for*

- 723            *Colorectal Cancer: A Systematic Review for the U.S. Preventive Services Task*  
724            *Force*. Rockville (MD): Agency for Healthcare Research and Quality (US); 2016.
- 725    32.    Zauber AG, Lansdorp-Vogelaar I, Knudsen AB, Wilschut J, van Ballegooijen M,  
726            Kuntz KM. Evaluating test strategies for colorectal cancer screening: a decision  
727            analysis for the U.S. Preventive Services Task Force. *Ann Intern Med*.  
728            2008;149(9):659-669.
- 729    33.    Weissfeld JL, Schoen RE, Pinsky PF, et al. Flexible sigmoidoscopy in the PLCO  
730            cancer screening trial: results from the baseline screening examination of a  
731            randomized trial. *J Natl Cancer Inst*. 2005;97(13):989-997.
- 732    34.    Johnson CD, Chen MH, Toledano AY, et al. Accuracy of CT colonography for  
733            detection of large adenomas and cancers. *N Engl J Med*. 2008;359(12):1207-  
734            1217.
- 735

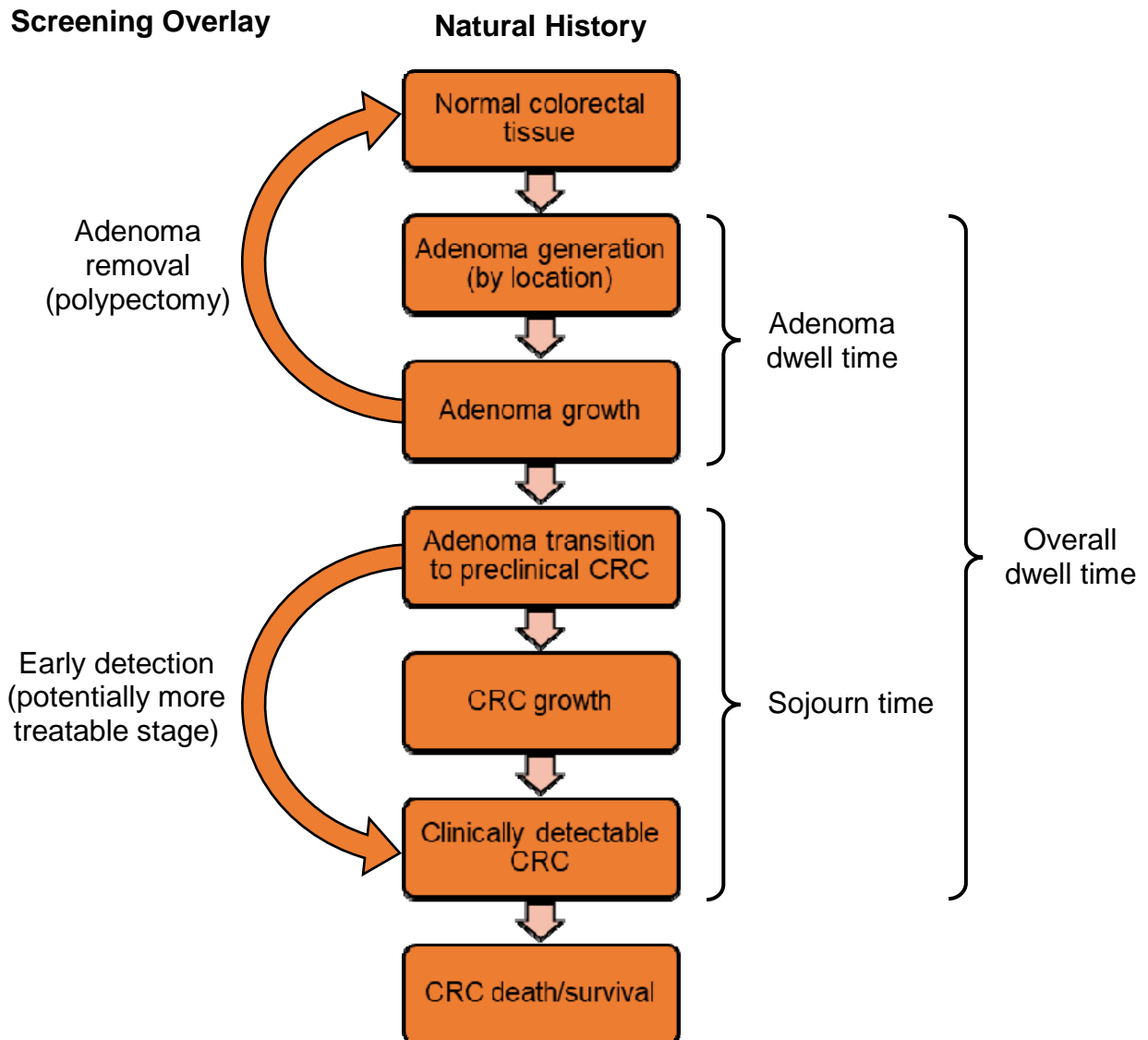
736 **Tables and Figures**

737

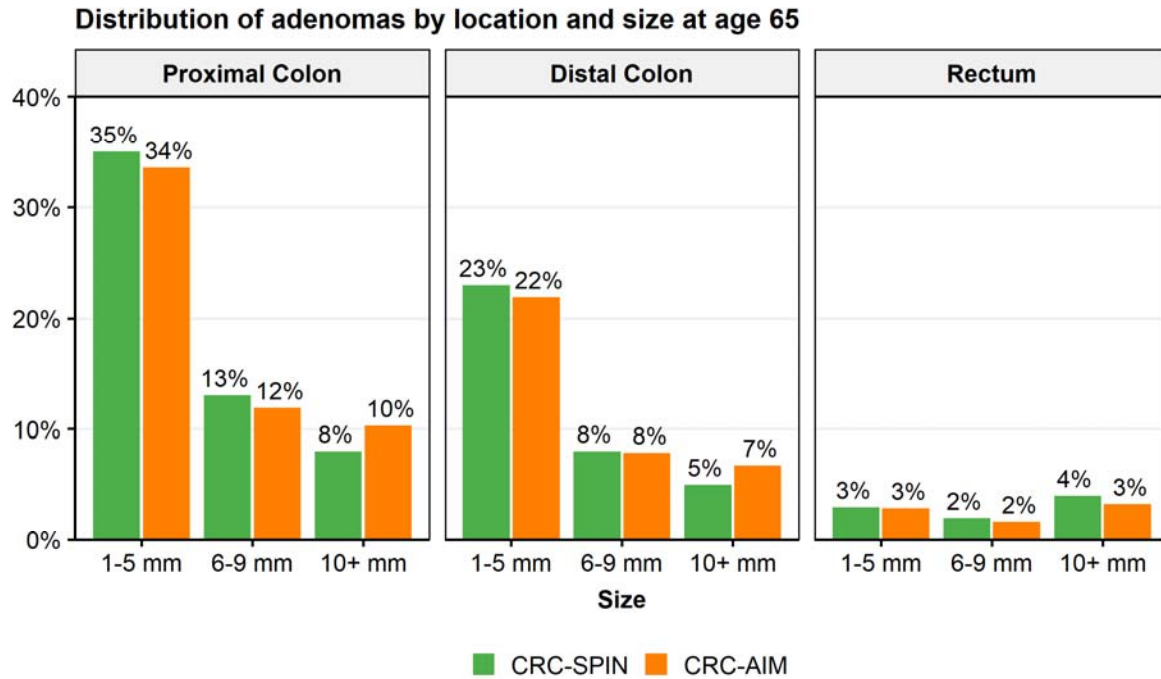
738 **Figure 1. Steps in the natural history of colorectal cancer (CRC) with description**  
739 **of screening consequences.**

740

741



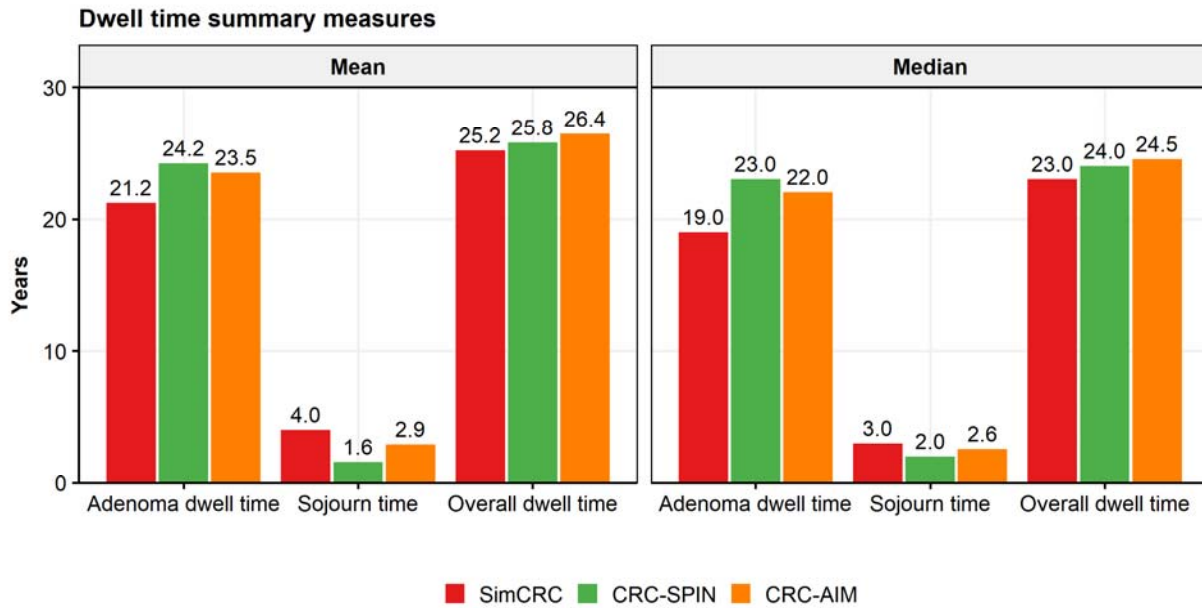
742 **Figure 2. Distribution of adenomas by size and location at age 65 in CRC-SPIN**  
743 **and CRC-AIM.** Sizes are subdivided into small (1-5 mm), medium (6-9 mm), and large  
744 (10+ mm) adenomas. Data adapted from Knudsen et al.<sup>21</sup>



745

746

747 **Figure 3. Median and mean adenoma dwell time, sojourn time, and overall dwell**  
748 **time in SimCRC, CRC-SPIN, and CRC-AIM.** Data adapted from Kuntz et al;<sup>12</sup> results  
749 from MISCAN are not included as the model has been subsequently recalibrated.

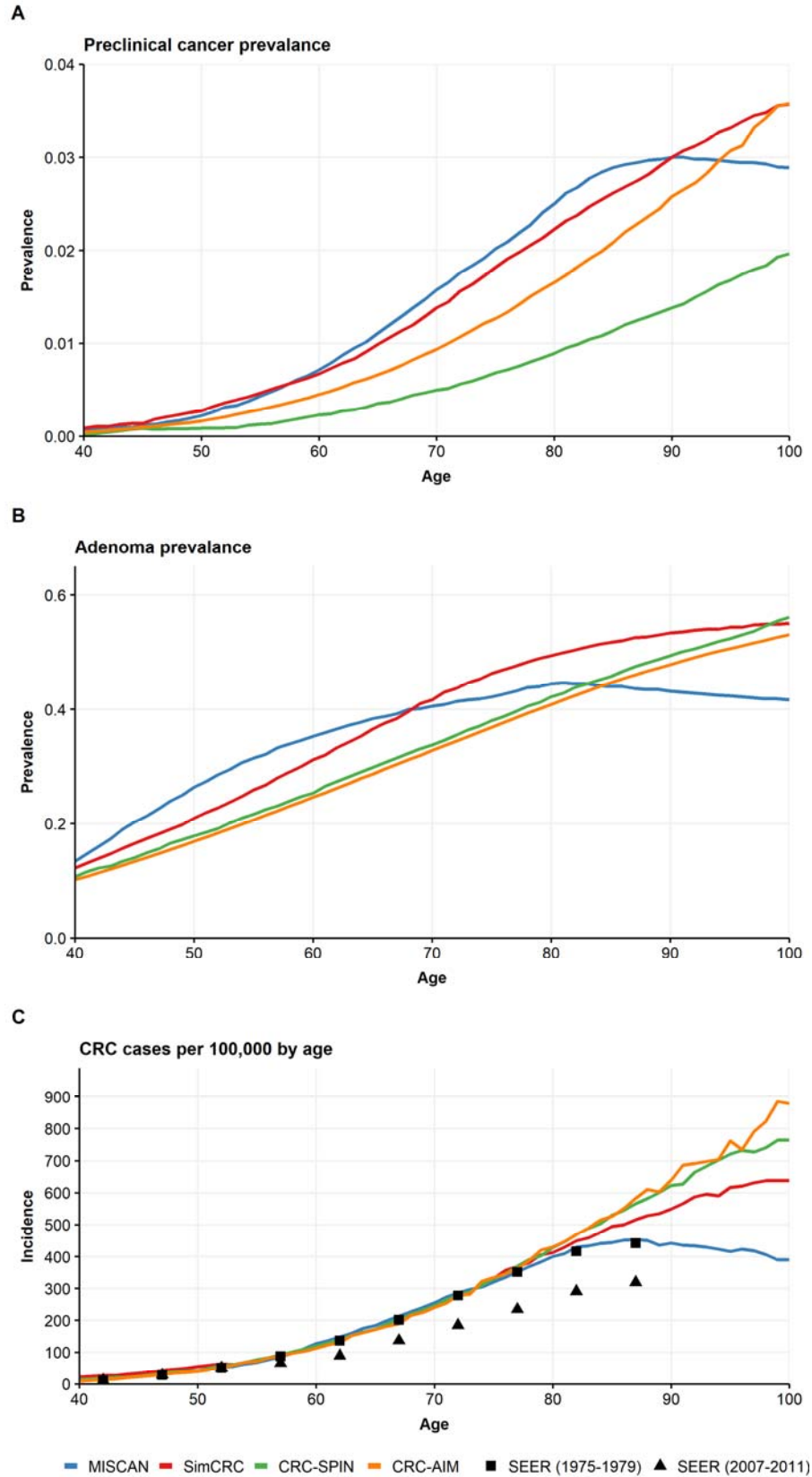


750

751

752 **Figure 4. Preclinical cancer prevalence, adenoma prevalence, and colorectal**  
753 **cancer (CRC) incidence by model.** Prevalence of (A) preclinical cancers and (B)  
754 adenoma by age. (C) Incidence of clinically diagnosed CRC per 100,000 individuals by  
755 age. Black squares represent CRC incidence for largely unscreened population  
756 according to the Surveillance, Epidemiology, and End Results data (SEER 1975-1979);  
757 black triangles represent CRC incidence with majority of screening-adherent individuals  
758 (SEER 2007-2011). Data adapted from Zauber et al.<sup>14</sup>  
759

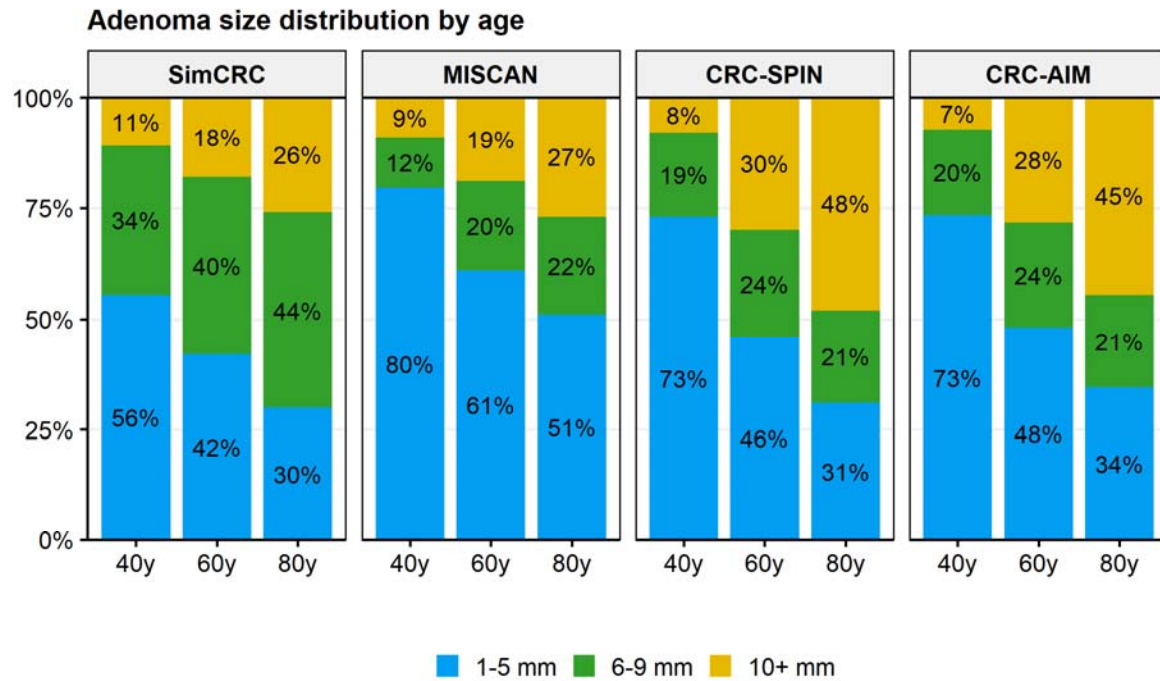




760

761

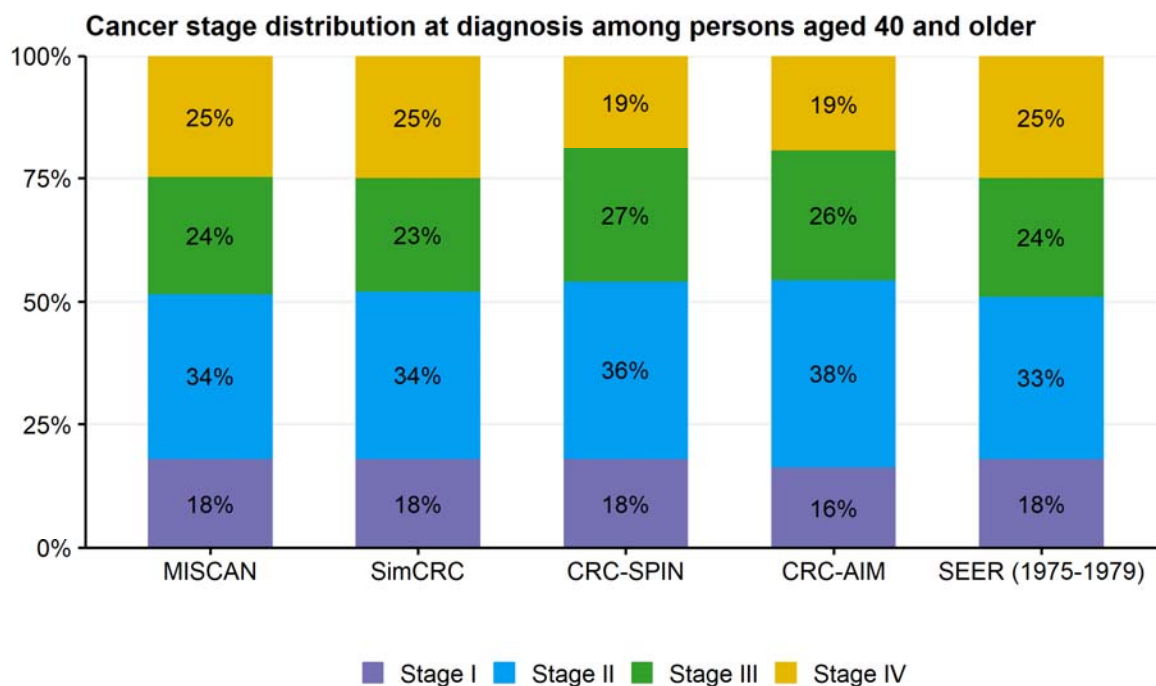
762 **Figure 5. Adenoma size distribution by age of the most advanced adenoma by**  
763 **model.** Data adapted from Zauber et al.<sup>14</sup>



764

765

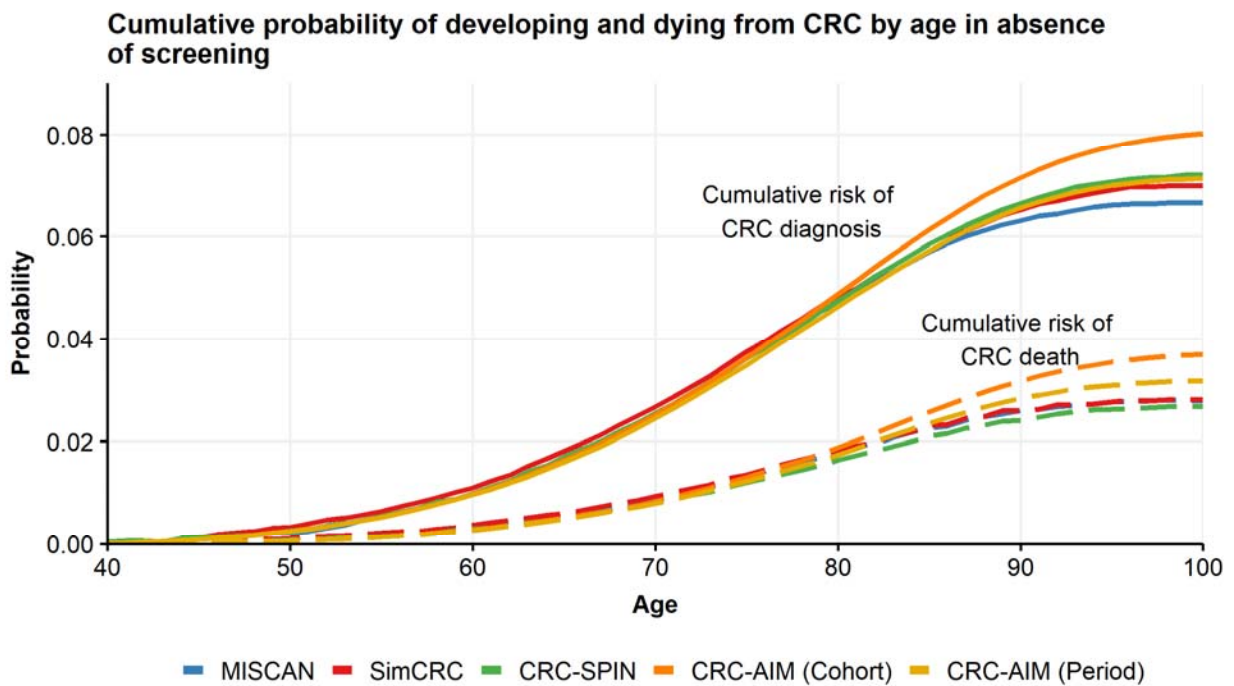
766 **Figure 6. Colorectal cancer (CRC) stage distribution at clinical diagnosis among**  
767 **individuals aged 40 or older by model.** Natural history stage distribution in the  
768 absence of screening is represented by Surveillance, Epidemiology, and End Results  
769 data (“SEER 1975-1979”). Stage was defined according to the American Joint  
770 Committee on Cancer (AJCC) staging system. Data adapted from Zauber et al.<sup>14</sup>



771

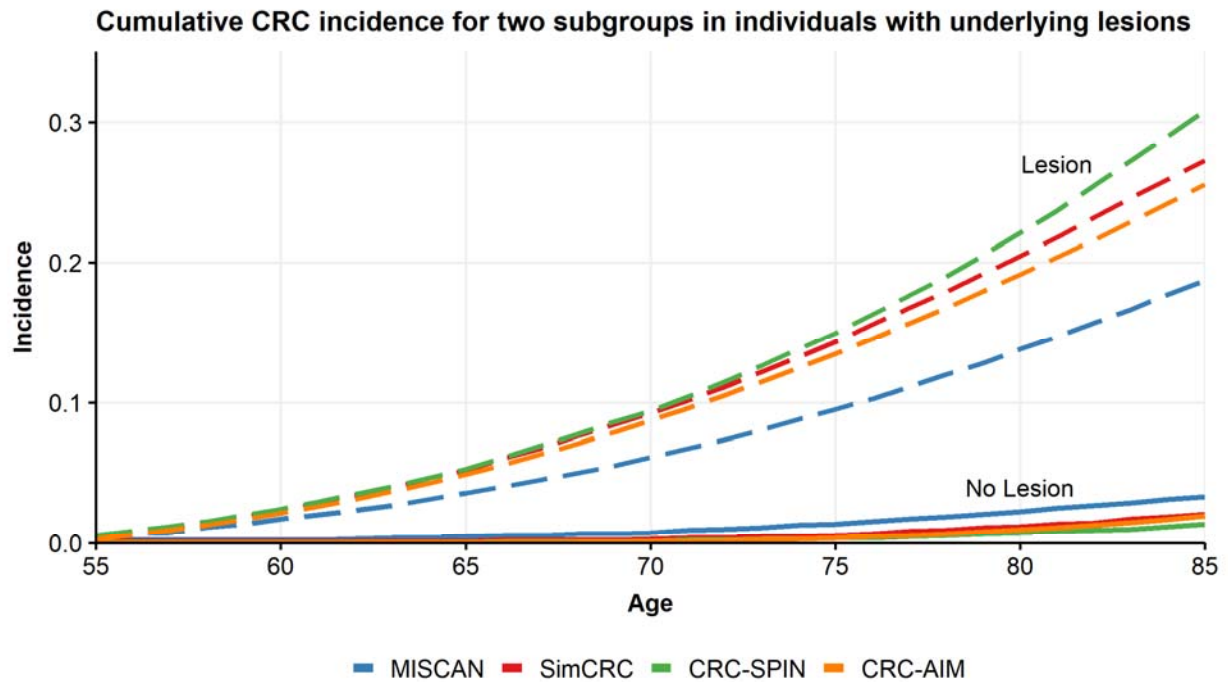
772

773 **Figure 7. Cumulative probability of developing and dying from colorectal cancer**  
774 **(CRC) in the absence of screening by model.** CRC-AIM results are displayed either  
775 using cohort life tables (“Cohort”), used standardly in CRC-AIM, or period life tables  
776 (“Period”), used in MISCAN, SimCRC, and CRC-SPIN, and for direct comparison in  
777 CRC-AIM. Data adapted from Zauber et al.<sup>14</sup>



778

779 **Figure 8. Cumulative CRC incidence for two subgroups in individuals with**  
780 **underlying lesions by model.** The subgroups include individuals with or without an  
781 adenoma or preclinical cancer at age 55 (“Lesion” or “No Lesion”, respectively). Data  
782 from Kuntz et al.<sup>12</sup>

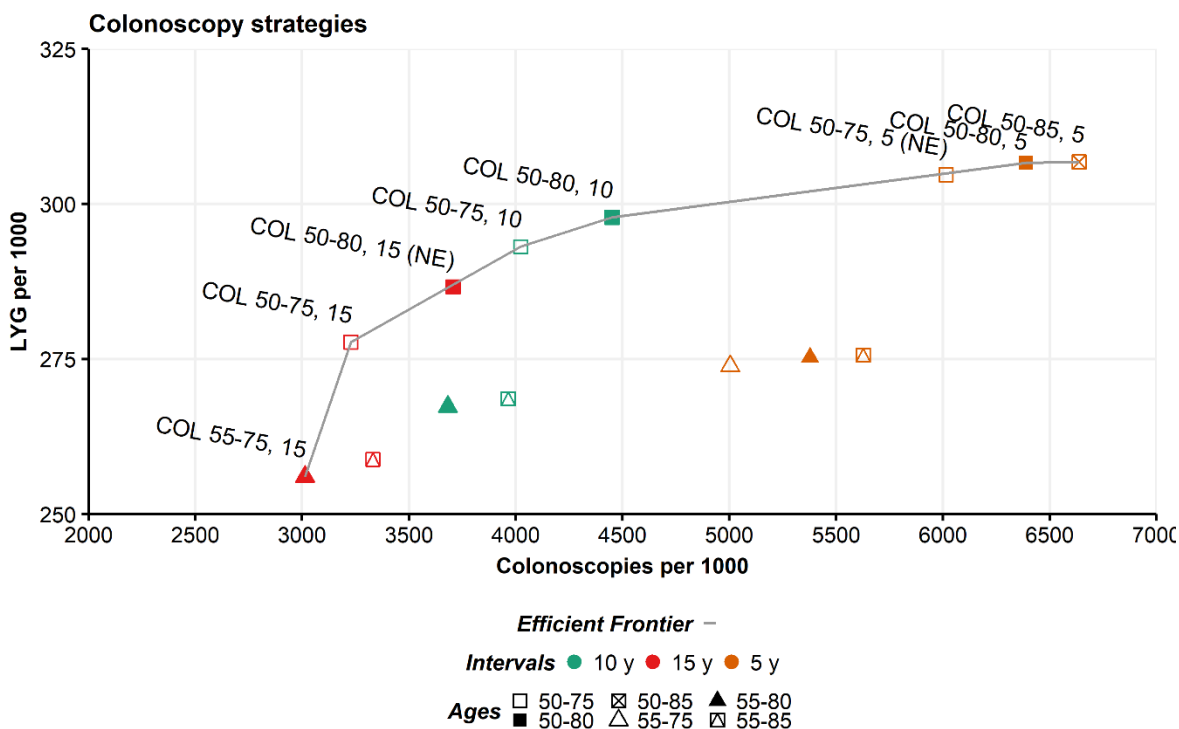


783

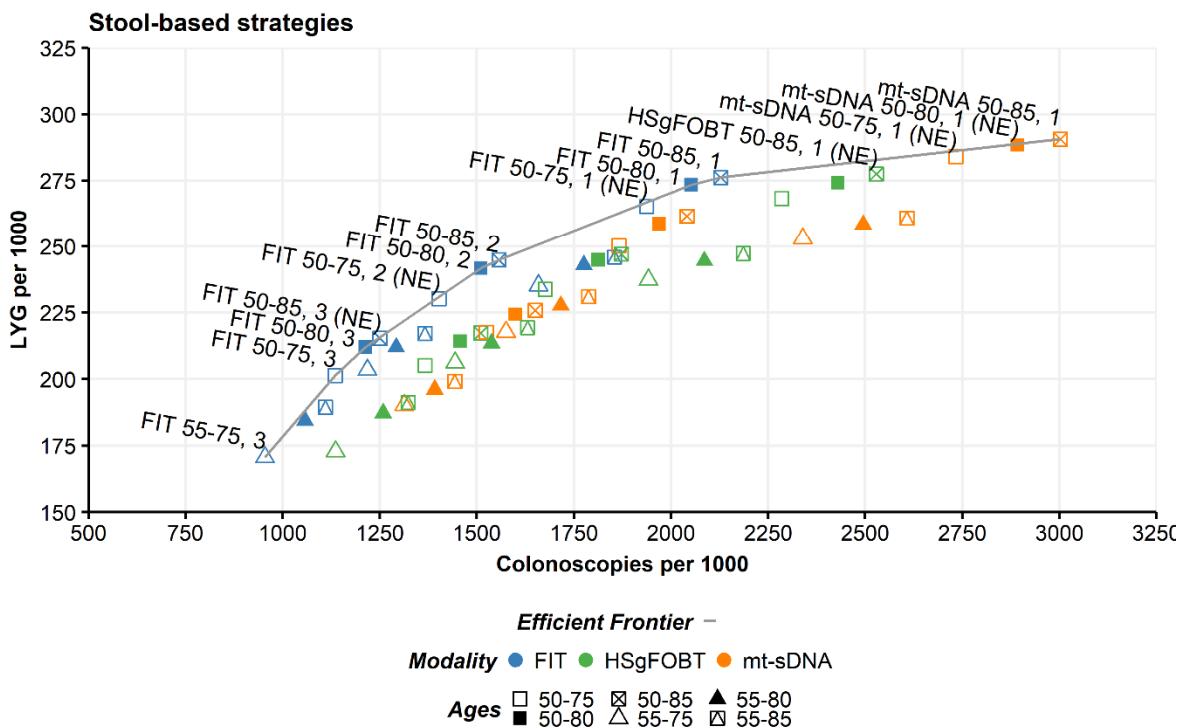
784

785 **Figure 9. Efficient frontier of screening strategies for individuals aged 40 years**  
786 **using (A) colonoscopy and (B) stool-based tests.** Models conformed to the CISNET  
787 assumption of perfect adherence. FIT, fecal immunochemical test; HSgFOBT, high  
788 sensitivity guaiac based fecal occult blood test; mt-sDNA, multi-target stool DNA. NE,  
789 near-efficient.

A



B



790

791

792 **Table 1. Prevalence and incidence of adenoma and colorectal cancer (CRC) by**

793 **model.** Multiplicity of adenomas data adapted from Kuntz et al<sup>12</sup>; other data adapted

794 from Knudsen et al.<sup>21</sup>

795 \*The table from Knudsen et al<sup>21</sup> labels this category as “1-10 mm”.

796 \*\*The maximum lifespan age was not explicitly mentioned in Knudsen et al.<sup>21</sup> CRC-AIM

797 simulation stop-age was 120 years.

Outcome		MISCAN	SimCRC	CRC-SPIN	CRC-AIM
Adenoma prevalence, age 65		39.80%	37.20%	30.70%	29.17%
Multiplicity of adenomas, age 65		2.0	1.6	1.8	1.7
Number of adenomas per 1000 by location/size at age 65					
Proximal Colon	1-5 mm	121.2	171.7	190.2	188.6
	6-9 mm	69.9	186.2	67.8	66.9
	≥10 mm*	61.8	23.9	40.8	57.8
Distal Colon	1-5 mm	134.4	124.2	124.5	123.3
	6-9 mm	77.4	18.2	44.4	44.2
	≥10mm	68.4	41.6	26.7	37.8
Rectum	1-5 mm	133.5	8.7	14.1	16.2
	6-9 mm	76.8	16.0	9.1	9.2
	≥10 mm	68.1	15.8	20.2	18.4
Adenoma distribution by location/size at age 65					
Proximal Colon	1-5 mm	15%	28%	35%	34%
	6-9 mm	9%	31%	13%	12%
	≥10 mm	8%	4%	8%	10%
	Total	31%	63%	56%	56%
Distal Colon	1-5 mm	17%	20%	23%	22%
	6-9 mm	10%	3%	8%	8%
	≥10 mm	8%	7%	5%	7%
	Total	35%	30%	36%	36%
Rectum	1-5 mm	16%	1%	3%	3%
	6-9 mm	9%	3%	2%	2%
	≥10 mm	8%	3%	4%	3%
	Total	34%	7%	8%	8%
Cumulative CRC incidence among cancer-free individuals at age 65					
10-year cumulative	Stage I	0.4%	0.4%	0.3%	0.4%



incidence	Stage II	0.7%	0.7%	0.7%	0.9%
	Stage III	0.5%	0.5%	0.5%	0.6%
	Stage IV	0.5%	0.5%	0.3%	0.5%
	Total	2.1%	2.2%	1.8%	2.3%
20-year cumulative incidence	Stage I	0.8%	0.8%	0.7%	0.8%
	Stage II	1.6%	1.5%	1.4%	1.8%
	Stage III	1.0%	1.0%	1.0%	1.2%
	Stage IV	1.0%	1.2%	0.7%	1.0%
	Total	4.4%	4.6%	3.9%	4.8%
Lifetime** cumulative incidence	Stage I	1.0%	1.0%	0.9%	1.1%
	Stage II	2.1%	2.0%	1.9%	2.4%
	Stage III	1.3%	1.4%	1.4%	1.7%
	Stage IV	1.3%	1.6%	1.0%	1.3%
	Total	5.7%	6.0%	5.3%	6.4%

798

799

800 **Table 2. Screening test characteristic inputs.** Reproduced and adapted with  
 801 permission from Knudsen et al, 2016.<sup>2</sup> CRC, colorectal cancer.

Screening Test	Value	Source
<b>Colonoscopy (within reach, per lesion)</b>		
Specificity	86% <sup>b</sup>	(2013) Schroy et al <sup>28</sup>
Sensitivity for adenomas 1-5 mm	75%	(2006) Van Rijn et al <sup>29</sup>
Sensitivity for adenomas 6-9 mm	85%	(2006) Van Rijn et al <sup>29</sup>
Sensitivity for adenomas ≥10 mm	95%	(2006) Van Rijn et al <sup>29</sup>
Sensitivity for CRC	95%	Assumed
Reach	95% (to end of cecum, remainder between rectum and cecum) <sup>c</sup>	Assumed
Risk of complications (serious/other gastrointestinal and cardiovascular)	age-specific risks <sup>d</sup>	(2014) Van Hees et al <sup>19</sup> ; (2009) Warren et al <sup>17</sup> ; (2003) Gatto et al <sup>18</sup>
<b>Fecal immunochemical test (per person)</b>		
Specificity	96.5%	(2014) Imperiale et al <sup>30</sup>
Sensitivity for adenomas 1-5 mm	7.6% <sup>e</sup>	(2014) Imperiale et al <sup>30</sup>
Sensitivity for adenomas 6-9 mm		(2014) Imperiale et al <sup>30</sup>
Sensitivity for adenomas ≥10 mm	23.8% <sup>f</sup>	(2014) Imperiale et al <sup>30</sup>
Sensitivity for CRC	73.8%	(2014) Imperiale et al <sup>30</sup>
Reach	whole colorectum	Assumed
Risk of complications	0%	(2016) Lin et al <sup>31</sup>
<b>High sensitivity guaiac based fecal occult blood test (per person)</b>		
Specificity	92.5%	(2008) Zauber et al <sup>32</sup>
Sensitivity for adenomas 1-5 mm	7.5% <sup>g</sup>	(2008) Zauber et al <sup>32</sup>
Sensitivity for adenomas 6-9 mm	12.4%	(2008) Zauber et al <sup>32</sup>
Sensitivity for adenomas ≥10 mm	23.9%	(2008) Zauber et al <sup>32</sup>
Sensitivity for CRC	70%	(2008) Zauber et al <sup>32</sup>
Reach	whole colorectum	Assumed
Risk of complications	0%	(2016) Lin et al <sup>31</sup>
<b>Multi-target stool DNA (per person)</b>		
Specificity	89.8%	(2014) Imperiale et al <sup>30</sup>
Sensitivity for adenomas 1-5 mm	17.2% <sup>e</sup>	(2014) Imperiale et al <sup>30</sup>
Sensitivity for adenomas 6-9 mm		(2014) Imperiale et al <sup>30</sup>
Sensitivity for adenomas ≥10 mm	42.4% <sup>f</sup>	(2014) Imperiale et al <sup>30</sup>
Sensitivity for CRC	92.3%	(2014) Imperiale et al <sup>30</sup>
Reach	Whole colorectum	Assumed
Risk of complications	0%	(2016) Lin et al <sup>31</sup>

<b>SIG Flexible sigmoidoscopy (within reach, per lesion)</b>		
Specificity	87% <sup>b</sup>	(2005) Weissfeld et al <sup>33</sup>
Sensitivity for adenomas 1-5 mm	75%	Assumed
Sensitivity for adenomas 6-9 mm	85%	Assumed
Sensitivity for adenomas ≥10 mm	95%	Assumed
Sensitivity for CRC	95%	Assumed
Reach	76-88% to sigmoid-descending junction; 0% beyond splenic flexure	(2003) Atkin et al <sup>15</sup> ; (1999) Painter et al <sup>16</sup>
Risk of complications	0%	Assumed <sup>h</sup> ; (2014) van Hees et al <sup>19</sup> ; (2009) Warren et al <sup>17</sup>
<b>CTC Computed tomographic colonography (CTC) (per lesion)</b>		
Specificity	88% <sup>i</sup>	(2008) Johnson et al <sup>34</sup>
Sensitivity for adenomas 1-5 mm	NPnot provided (only individuals with ≥6 mm lesions are determined to have positive CTC tests)	(2008) Johnson et al <sup>34</sup>
Sensitivity for adenomas 6-9 mm	57%	(2008) Johnson et al <sup>34</sup>
Sensitivity for adenomas ≥10 mm	84%	(2008) Johnson et al <sup>34</sup>
Sensitivity for CRC	84%	(2008) Johnson et al <sup>34</sup>
Reach	Whole colorectum	Assumed
Risk of complications	0%	(2016) Lin et al <sup>31</sup>

802

803

804 **Table 3. Percent of adenomas that had developed within 10 years or 20 years of**  
805 **clinical colorectal cancer diagnosis by model.** Data adapted from Kuntz et al.<sup>12</sup>

Age at cancer diagnosis (years)	Adenomas developed (%)			
	MISCAN	CRC-SPIN	SimCRC	CRC-AIM
Within 10 years of clinical cancer diagnosis				
55	72%	3%	10%	6.5%
65	67%	4%	9%	6.7%
75	62%	4%	9%	7.5%
Within 20 years of clinical cancer diagnosis				
55	94%	24%	39%	42.2%
65	92%	25%	37%	37.5%
75	89%	28%	33%	36.2%

806

807

808 **Table 4. Screening strategies evaluated at perfect adherence.** COL, colonoscopy;  
 809 CTC, computed tomographic colonography; FIT, fecal immunochemical test; HSgFOBT,  
 810 high sensitivity guaiac based fecal occult blood test; mt-sDNA, multi-target stool DNA  
 811 test; SIG, flexible sigmoidoscopy

812

Screening Modality	Screening Interval, y	Age to Begin Screening, y	Age to End Screening, y	No. of (Unique) Strategies
no screening	NA	NA	NA	1 (1)
COL	5, 10, 15	45, 50, 55	75, 80, 85	27 (20)
mt-sDNA	1, 3, 5	45, 50, 55	75, 80, 85	27 (27)
FIT	1, 2, 3	45, 50, 55	75, 80, 85	27 (27)
HSgFOBT	1, 2, 3	45, 50, 55	75, 80, 85	27 (27)
SIG	5, 10	45, 50, 55	75, 80, 85	18 (15)
SIG and FIT (SIG_FIT)	5_2, 5_3, 10_1, 10_2	45, 50, 55	75, 80, 85	36 (36)
SIG and HSgFOBT (SIG_HSgFOBT)	5_2, 5_3, 10_1, 10_2	45, 50, 55	75, 80, 85	36 (36)
CTC	5, 10	45, 50, 55	75, 80, 85	18 (15)

813